

Floquet engineering the quantum Rabi model in the ultrastrong coupling regime

Kamran Akbari,^{1,*} Franco Nori,^{2,3,4} and Stephen Hughes¹

¹*Department of Physics, Engineering Physics and Astronomy,
Queen's University, Kingston ON K7L 3N6, Canada*

²*Theoretical Quantum Physics Laboratory, Cluster for Pioneering Research, RIKEN, Wakoshi, Saitama 351-0198, Japan*

³*Quantum Computing Center, RIKEN, Wakoshi, Saitama, 351-0198, Japan*

⁴*Physics Department, The University of Michigan, Ann Arbor, Michigan 48109-1040, USA*

(Dated: July 24, 2024)

We study the quantum Rabi model for a two-level system coupled to a quantized cavity mode under periodic modulation of the cavity-dipole coupling in the ultrastrong coupling regime, leading to rich Floquet states. As an application of the theory, we show how purely mechanical driving can produce real photons, depending on the strength and frequency of the periodic coupling rate.

Since the early observations with intersubband polaritons [1, 2], the ultrastrong coupling (USC) regime of light-matter interactions has emerged as a fascinating and distinctive phenomenon in quantum optics, particularly within the realm of cavity quantum electrodynamics (QED) [3, 4]. A particularly intriguing facet of USC is the occupation of virtual excitations (e.g., photons), even in the ground state of the dressed system, which is a consequence of counter-rotating wave effects and breaking $U(1)$ symmetry [3, 5]. This raises the question of whether it is possible to convert virtual photons into real ones [3, 6], which requires input energy, e.g., coherent/incoherent excitation [7, 8], to introduce time-dependent characteristics into the system, nonadiabatically [9, 10].

Although virtual excitations are not detectable, ideas have been proposed to release them as real excitations [7–9, 11–27]. These methods typically involve modulating one of the system parameters [7, 9, 13–21, 26, 27], e.g., time-modulation of the Rabi frequency [9, 13], using flying atoms [27], and exploiting phonon pumping [26, 28]. Nevertheless, the first theory proposals [29–31] that paved the way to the successful experiments [32, 33] (particularly, in circuit QED) were mostly associated with the dynamical Casimir effect [28, 34–36].

The quantum Rabi model (QRM), where a two-level system (TLS) is coupled to a single quantized cavity mode, is the key model in cavity-QED. In USC, there is a prominent role played by counter-rotating wave effects and ponderomotive energies, and the Jaynes-Cummings model, a cornerstone rotating-wave model for explaining weak and strong coupling effects, is no longer valid [37–39]. Instead, one must consider the joint atom-cavity dressed states [3, 38–40], where even the ground state is an entangled state of photons and matter. Moreover, it is essential to uphold the gauge-invariance principle when dealing with truncated matter models [37–39, 41–45].

However, for driven cavity-QED systems, the QRM can also fail, since the strong hybridization of the bare subsystems, demands a nonperturbative treatment [38, 40] before and after driving. Often, periodic driving is considered as a weak perturbation that induces transitions between the (pre-driving) hybrid states [38, 46].

Yet, when the strength of the driving amplitude is also significant, the dressed (joint) light-matter states of the entire system transforms into a Floquet picture, an important theoretical framework for understanding periodically driven systems [47, 48]. Apart from fundamental interest, Floquet theory is a powerful tool for engineering quantum systems [48–59] and reservoirs [60, 61], and has been used for describing photon-assisted quantum tunneling/transport [48, 62–67]. To the best of our knowledge, it has not been utilized for the USC regime.

In this work, we describe how one can *Floquet engineer the QRM*, by applying nonperturbative periodic oscillations to the TLS-cavity coupling rate. The hybrid system states evolve nonadiabatically into Floquet quasienergy states, forming new transitions via the newly-introduced anticrossings in the Floquet picture. This type of periodic modulation can connect to various experimentally accessible regimes, such as the dynamical Casimir effect [28], surface acoustic waves in semiconductors [68, 69], and optomechanical interactions [8], including molecular optomechanics [70–72]. Our significant findings include: (i) a double-field (photon plus mechanical oscillation)-assisted splitting of the QRM states due to the renormalization of the time-independent energy states, (ii) production of real photons and TLS excitations from vacuum, (iii) higher-order nonlinear quantum processes that are effective only in the USC regime.

We begin with the *time-dependent* QRM Hamiltonian,

$$\mathcal{H}_{\text{FQR}}(t) = \omega_c a^\dagger a + \frac{\omega_a}{2} \{ \sigma_z \cos[c(t)] + \sigma_y \sin[c(t)] \}, \quad (1)$$

in the Coulomb gauge [41] ($\hbar=1$), where ω_c (ω_a) is the cavity (TLS) transition frequency, a (a^\dagger) is the cavity photon annihilation (creation) operator, σ_i are the TLS Pauli operators, and $c(t) = 2(a + a^\dagger)\eta(t)$. The normalized TLS-cavity coupling rate is $\eta(t) = \eta_0 + \eta_M \sin(\omega_M t)$, where $\eta_0 \equiv g/\omega_c$ is the normalized time-independent coupling rate (g is the atom-cavity coupling rate), and η_M is the amplitude of the time-dependent coupling, with ω_M the frequency of the driven time-dependent oscillation. The calligraphic notation of the Hamiltonian in-

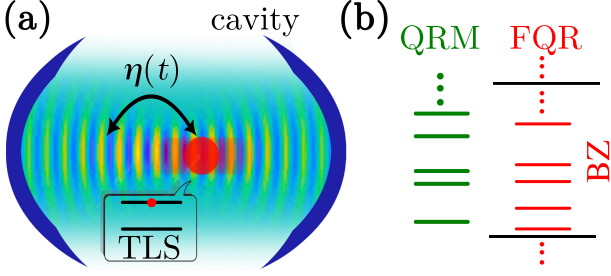


Figure 1. (a) Schematic of a TLS with a mechanical vibration inside a cavity with a dominant single mode. (b) Without the mechanical vibration, the system is identified by the usual (time-independent) QRM Hamiltonian with N_j dressed states (left); after the periodic vibration is turned on, the Floquet quasi-energies and states (FQR) govern the system (right) transitions, with N_j of them in one Brillouin zone (BZ).

indicates that the gauge-fixed Hamiltonian is used for the *truncated* matter Hilbert space [38, 41, 45]. Note that when $\eta(t) \rightarrow \eta$, then Eq. (1) fully recovers previous time-independent (and gauge invariant) models [38, 39, 41]. Figure 1 shows a schematic of our time-dependent QRM.

Due to the periodicity of the time-dependent coupling, with period $T = 2\pi/\omega_M$, the Hamiltonian is also periodic: $\mathcal{H}_{\text{FQR}}(t) = \mathcal{H}_{\text{FQR}}(t + T)$, which can be expanded as a Fourier series $\mathcal{H}_{\text{FQR}}(t) = \sum_{m \in \mathbb{Z}} \mathcal{H}_m e^{im\omega_M t}$, with

$$\mathcal{H}_m = \omega_c a^\dagger a \delta_{m0} + \frac{\omega_a}{2} \left\{ \frac{\sigma_z - i\sigma_y}{2} e^{i2(a+a^\dagger)\eta_0} + (-1)^m \frac{\sigma_z + i\sigma_y}{2} e^{-i2(a+a^\dagger)\eta_0} \right\} J_m[2(a+a^\dagger)\eta_M], \quad (2)$$

where J_m is the Bessel function of the first kind of order m , and we have used the Anger-Jacobi expansion [73] of Eq. (1). When $\eta_M \rightarrow 0$, then $J_0(0) = 1$ and $J_{m \geq 0}(0) = 0$, and we recover the time-independent QRM Hamiltonian. In practice, we must also truncate $|m| \leq m_{\max}$. Note also that \mathcal{H}_m separates into a time-independent part for $m = 0$ (including a shift due to $\eta_M \neq 0$), and a time-dependent interaction (for $m \neq 0$). Thus, while η_M is related to the time-dependent light-matter interaction, there is a static contribution from the J_0 term. While Hamiltonian (1) accounts for the static dressing via photon-matter interactions, Eq. (2) *dresses* the entire cavity-QED system with periodic mechanical oscillations. Similar expressions are widely considered for single quantum systems, including field-driven TLSs [74].

For numerical calculations, the time-independent \mathcal{H}_0 , is first diagonalized with the eigenbasis $\{E_j, |j\rangle\}_{j=0}^{N_j-1}$, where N_j is the number of truncated AC-shifted QR-dressed states, obtained from $\mathcal{H}_0|j\rangle = E_j|j\rangle$, which satisfies the conditions $\langle j|j'\rangle = \delta_{jj'}$ and $\sum_{jj'} |j\rangle\langle j'| = \mathbf{1}$; here E_j ($|j\rangle$) are shifted QRM eigenenergies (eigenstates) renormalized by the presence of the nonzero η_M , since the time-independent portion of the Hamiltonian is \mathcal{H}_0 , and

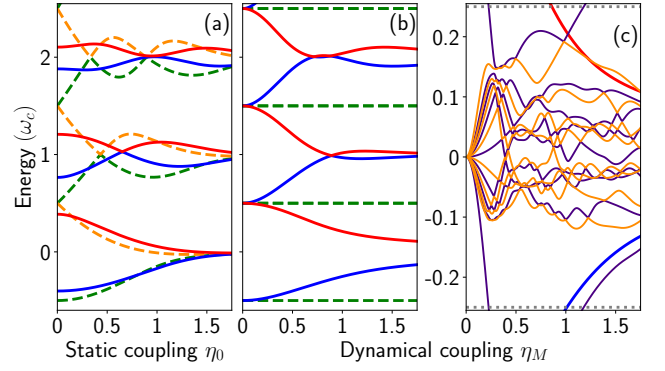


Figure 2. (a) Eigenenergies obtained from Eq. (2) for $m = 0$ with $\eta_M = 0$ (QRM, dashed curved), and for $\eta_M = 0.5$ (solid lines), versus η_0 . (b) Eigenenergies obtained from Eq. (2) again for $m = 0$ (i.e., static part), but now as a function of finite η_M (solid lines), with $\eta_0 = 0$, as well as the QRM eigenenergies (dashed lines). (c) Floquet quasienergies in the 1st BZ for $\eta_0 = 0$, versus η_M . Thin solid (with every other indigo and dark orange color to show anticrossings) lines represent different Floquet quasienergies. Thicker blue (lower) and red (upper) curves are the first two shifted eigenenergies from panel (b). The parameters used are: $\omega_M = 0.5\omega_c$, $\omega_a = \omega_c$, $N_j = 16$, $m_{\max} = l_{\max} = 20$ (see text).

not $\mathcal{H}_{\text{QRM}} = \omega_c a^\dagger a + (\omega_a/2)\{\sigma_z \cos[c(0)] + \sigma_y \sin[c(0)]\}$. This also ensures that we use the correct static states of the joint light-matter system in the presence of driving.

Solving the time-dependent Schrödinger equation, $i\partial_t|\psi(t)\rangle = \mathcal{H}_{\text{FQR}}(t)|\psi(t)\rangle$, yields $|\psi_\alpha(t)\rangle = e^{-i\varepsilon_\alpha t}|\alpha(t)\rangle$, where ε_α is the Floquet quasienergy [75], and the Floquet mode $|\alpha(t)\rangle$ is T -periodic [47, 76]. The Floquet Hamiltonian, $\mathcal{H}_F(t) \equiv \mathcal{H}_{\text{FQR}}(t) - i\partial/\partial t$, is associated with a set of quasienergies $\{\varepsilon_\alpha\}$. The Floquet states, $\{|\psi_\alpha(t)\rangle\}$, form a complete basis for any value of t , thus $|\psi(t)\rangle = \sum_\alpha c_\alpha |\psi_\alpha(t)\rangle$, where $c_\alpha = \langle \alpha|\psi(0)\rangle$, with $|\alpha\rangle \equiv |\alpha(0)\rangle$. Transition resonances occur at differences between Floquet energies [77]. To compute the Floquet modes, we use a Fourier series expansion of $|\alpha(t)\rangle = \sum_{l \in \mathbb{Z}} e^{il\omega_M t} |\alpha_l\rangle$, where the Fourier coefficient states $|\alpha_l\rangle$ are *Floquet sidebands*. There are N_j quasienergies confined within a $[-\omega_M/2, \omega_M/2]$ energy range (first BZ), associated with N_j linearly independent Floquet modes [78].

In Fig. 2(a), we plot the eigenenergies versus η_0 , from the *time-independent* part of the total Hamiltonian in Eq. (1), i.e., using \mathcal{H}_0 from Eq. (2), for a fixed value of $\eta_M = 0.5$ (solid curves), and show how these compare with the standard QRM (dashed curves). This demonstrates how time-modulation introduces an effective static (DC) dressing of the QRM eigenenergies. Also, we note from the form of the solid curves, that the levels are initially split, i.e., at $\eta_0 = 0$, with more significant splittings for higher energy levels. As η_0 increases, we then enter a regime of *double dressing*.

In Fig. 2(b), we show the eigenenergies of the *time-independent* part of the total Hamiltonian in Eq. (1),

characterized by \mathcal{H}_0 in the expansion terms in Eq. (2), in comparison with the eigenenergies of the QRM, versus η_M , for $\eta_0 = 0$. There is a shifting (renormalization) of the eigenenergies, and then a modified anticrossing of the time-independent (static) eigenenergies. We also recognize that as one transitions toward the USC (i.e., $\eta_M > 0.1$), the shifts are amplified until they form new anticrossing regions. Note these shifts are independent of the ω_M . When $\eta_0 = \eta_M = 0$, there is no QRM dressing and no hybridization between the light and matter states [dashed green lines in panel 2(b)]. By increasing the static coupling $\eta_0 > 0$ when $\eta_M = 0$ [dashed lines in panel 2(a)], the light-matter hybridization begins, where the states are closer to each other, e.g., the first excited state is pushed closer to the ground state, and the second and third excited states move closer. As η_M increases, this boosts the hybridization in such a way that they form new anticrossings at certain field strengths, which depends on the state levels.

We next transform the problem to the Floquet picture, including the various m solutions. In Fig. 2(c), the Floquet quasienergies within the 1st BZ are shown for the QRM truncated with sixteen states, so that at each value of the drive's parameters there exist (nominally) sixteen quasienergy states within one BZ. Although the original initial-time states are the QRM states, the Floquet states are built upon the renormalized states from the dynamical coupling. The DC component alters the transition selection rule between dressed states and induces significant intermixing of the QRM states. Due to the greater number of strongly coupled nearby states in the DC-renormalized Hamiltonian, nonlinear optical effects can occur at a much lower dynamical coupling strength than they would be in the absence of the DC coupling, strongly enhancing the transition probabilities [79–81]. This manifests in a rich Floquet quasienergy diagram, shown in Fig. 2(c), which yields a large number of anticrossings [80–85]. These quasienergies are continuous functions of the drive amplitude that shows avoided crossings, if there are no symmetries that allow crossings.

To help appreciate the dynamically-modified transitions, consider the QRM ground state at $t = 0^+$. As time evolves, with $\eta_M \neq 0$, the ground state adiabatically transforms into a Floquet state. At the first anticrossing between a Floquet sideband of the lower state and a Floquet sideband of a higher state, where a superposition of the Floquet sidebands is constructed, a diabatic transition, namely, $|\alpha_l\rangle \rightarrow |\alpha'_l\rangle$ at the anticrossing where a superposition $a|\alpha_l\rangle + a'|\alpha'_l\rangle$ is provided. Then, the created superposition, generally oscillating at a multiple of the stimulation frequency $\Delta\varepsilon = n\omega_M$, adiabatically transforms into the superposition of the two original QRM states, and now oscillates at their energy difference, $E_{kj} = E_k - E_j$. Depending on the size of ω_M , one can go back and forth among different BZs to form a transition between the QRM states, if it is parity allowed.

In the USC regime, transitions are not between the bare states of the system (with fixed numbers of photons and atomic excitations), but between the *dressed states of the composite system*. Indeed, naively assuming the emitted radiation is proportional to the photon population in the cavity leads to the prediction of unphysical radiation from the ground state in vacuum [17, 27, 38, 45]. Instead, one must use the correct dressed system operators [38, 40]

$$s^{\Lambda+} = \sum_{j,k>j} S_{jk}^{\Lambda} |j\rangle\langle k|, \quad (3)$$

where $s^{\Lambda-} = [s^{\Lambda+}]^\dagger$, with $\Lambda = \{\text{cav}, \text{TLS}\}$ and $S_{jk}^{\Lambda} \equiv \langle j|S^{\Lambda}|k\rangle$ is the matrix element of the system operator in the Schrödinger picture. Specifically, we use $S^{\text{cav}} = a(1+i)/\sqrt{2} + \text{H.c.}$ [86], and $S^{\text{TLS}} = \sigma_x$.

Next, we study how one can produce real photons from the *time-dependent* perturbation. We assume that the system is initially in the dressed ground state $|j=0\rangle$, and neglect thermal excitations. The number of real photon or TLS excitations are defined from [27, 38, 40] $N_{\Lambda}(t) = \langle \psi(t)|s^{\Lambda-}s^{\Lambda+}|\psi(t)\rangle$. In contrast, the virtual photon number in the ground state of the time-independent light-matter Hamiltonian is [5, 27] $\langle 0|a^\dagger a|0\rangle_{\text{QR}}$, which is nonzero in vacuum USC [3, 5]. An observable, $\langle \psi(t)|O|\psi(t)\rangle$, is not necessarily time periodic due to the presence of off-diagonal terms in the Floquet eigenbasis [87], $e^{i(\varepsilon_{\alpha}-\varepsilon_{\beta})(t-t_0)}\langle \alpha(t)|O|\beta(t)\rangle$, for $\alpha \neq \beta$ (see Fig. S3 in [78]). However, in real open systems, the off-diagonal terms are suppressed, and the time evolution of observables often becomes periodic with the same periodicity as the driving field. We thus add a phenomenological damping rate, γ , to the non-diagonal terms, which are then damped out after a sufficiently long time [5, 81, 87]. Subsequently, we derive the expectation values,

$$N_{\Lambda}(t) = \sum_{\alpha\beta} c_{\alpha}^* c_{\beta} e^{i(\varepsilon_{\alpha}-\varepsilon_{\beta})t-\gamma t(1-\delta_{\alpha\beta})} \langle \alpha(t)|s^{\Lambda-}s^{\Lambda+}|\beta(t)\rangle, \quad (4)$$

and obtain the steady-state values: $N_{\Lambda}(t > t_{\text{ss}}) = \sum_{\alpha} |c_{\alpha}|^2 \langle \alpha(t)|s^{\Lambda-}s^{\Lambda+}|\alpha(t)\rangle$. The mean real excitation number is $\bar{N}_{\Lambda} = \frac{1}{T} \int_{t_{\text{ss}}}^{t_{\text{ss}}+T} dt N_{\Lambda}(t)$, where T is sufficiently long to yield a steady-state average. Our result is exactly T periodic, so we only have to use one period.

In Fig. 3, we show $N_{\text{cav},\text{TLS}}(t)$, with zero static coupling, $\eta_0 = 0$, with different dynamical values of (a,b) $\eta_M = 0.2, 0.5$, using $\omega_M = 0.5\omega_c = 0.5\omega_a$. We note that the onset and time range of the periodic behavior of the populations after they reach the steady state are different for different values of the coupling. The results are periodic after a sufficiently long time, depending on the strength and frequency of dynamical coupling; we safely define $t_{\text{ss}} \sim 5T$. For increasing coupling, the periodic modulation causes a significant population of real photons (solid curves) and TLS excitation (dashed curves).

This scenario requires $\eta_M \neq 0$ and the USC regime. Note that the populations of the cavity are different to the TLS for increasing η_M , as the nonlinear behavior of the TLS and cavity photons are different for increasing drives.

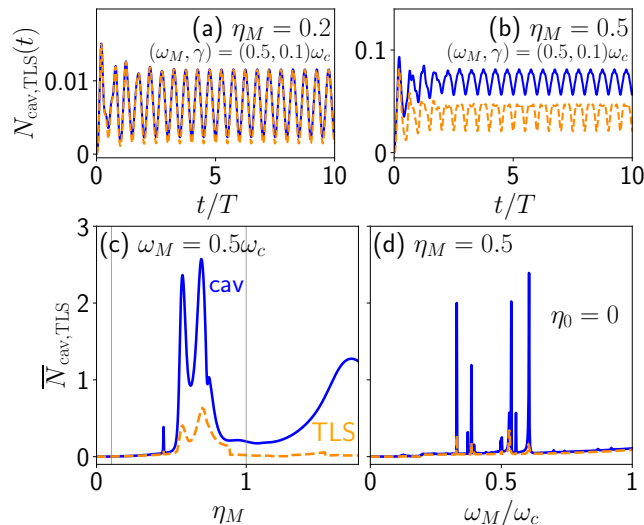


Figure 3. An example of the time-dependent real excitations, $N_{\text{cav}}(t)$ (real photons, solid blue line) and $N_{\text{TLS}}(t)$ (real TLS excitation, dashed orange line), given by Eq. (4), are shown for (a) $\eta_M = 0.2$ and (b) $\eta_M = 0.5$, with $\gamma = 0.1\omega_c$. Also, depicted are the *mean excitation numbers* that are the temporal average of the cavity excitation number, \bar{N}_{cav} (solid blue line) and the TLS excitation number, \bar{N}_{TLS} (dashed orange line), versus the amplitude (c) and frequency (d) of the dynamical coupling. The parameters used are: $\eta_0 = 0$, $\omega_a = \omega_c$ and $m_{\text{max}} = l_{\text{max}} = 20$. The grey vertical at $\eta_M = 0.1$ and $\eta_M = 1$ in panel (c) span the USC to deep-USC regime.

In Fig. 3(c), we plot the average real excitation numbers, versus η_M , with $\omega_M = 0.5\omega_c$ and $\eta_0 = 0$. Finite η_0 simulations are discussed in the supplement [78]. We also observe that the onset of USC (or switching on/off within the USC, i.e., the joint effect of the static and dynamical couplings) coincides with the starting point of turning virtual photons into real ones, where there exists the discrepancy between real and virtual photons [27], i.e., $\eta_M \geq 0.1$, since $\eta_0 = 0$. In Fig. 3(d), we plot the variation of the mean real excitation number versus ω_M , with a fixed $\eta_M = 0.5$, for the cavity (solid blue) and the TLS (dashed orange) excitations. From panel (d), we generally understand that because the switching on/off process is already in the USC, namely, because $\eta_M > 0.1$, the starting point of turning virtual photons into real ones begins as soon as $\omega_M > 0$, where we also observe a difference between the real photons and the TLS excitations, which is also higher when the amplitude and frequency of the mechanical motion are larger.

The results in Fig. 3(c,d) are obtained for sixteen QRM states and $m_{\text{max}} = l_{\text{max}} = 20$. Adding more truncated QRM states may modify some of the frequency/coupling

peaks, and add additional sharper peaks, but in practice these will be broadened with dissipation processes. Importantly, our main predictions are not qualitatively affected by a further increase in basis size. The general intuitive behavior of the spectral shape is that as the amplitude and frequency of the dynamical coupling increase within the USC range, and the number of real photons and TLS excitations become larger because of the enhanced nonlinearity of the quantum processes.

The peak and valley structures seen in Fig. 3(c,d) are connected to the anticrossings of the Floquet quasienergy spectrum. Moreover, higher multi-oscillation peaks are narrower than lower-oscillation peaks and they form earlier (smaller values) in amplitude and frequency of the drive. This general effect of an increasing spectral width of an absorption line with the increase in the steady source intensity is similar to the power broadening effect in atomic absorption spectra [88].

To highlight some general features, the major cavity double-peak and valley structure in Fig. 3(c) is actually formed by the combination of a $3-\omega_M$ resonance transition (from $|j=0\rangle \rightarrow |j=3\rangle$) and a $15-\omega_M$ resonance transition (from $|j=0\rangle \rightarrow |j=15\rangle$). In the first BZ of the quasienergy diagram [Fig. 1(c) and S2(b)], the most effective corresponding anticrossing (which is quite wide as well due to nonlinear effects of power broadening) at the same points between the two Floquet sidebands $|\alpha_l = 12_l\rangle$ and $|\alpha_l = 14_l\rangle$ (see Fig. S2 of supplement [78]). Furthermore, the very wide power-broadened peak at the far right of the panel is a $4-\omega_M$ peak due to the transition from the ground state to the fourth excited state.

Note that not only the creation of each individual peak, but also the interplay between the different order transitions and peaks are crucial in the overall construction and understanding of the population spectra. These interplays include the constructive and destructive nonlinear interaction of peaks with various widths and strengths, which can cause a sudden dip or rise, and nonlinear effects [81, 89–92] such as power broadening, dynamical Stark shift, Autler–Townes multiplet splitting, electromagnetically induced transparency, and hole burning. For example, the drop at $\eta_M \sim 0.9$ of the TLS graph in Fig. 3(c) is caused by the destructive interfering of transitions. These modifications arise due to Stark splitting of the driven system energy levels where the decaying system process (atomic down transition in the dressed states) from the two dressed states interferes destructively to create a Fano-type dark line in the single Lorentzian peak [79–81, 90]. Similar explanations are applicable for other resonant peaks in the same graph as well as those in Fig. 3(d), which shows the role of increasing ω_M for fixed $\eta_M = 0.5$ [78].

Lastly, we comment on the role of the $\eta(t)$ waveform. With a pure harmonic $\eta(t)$ waveform, one can drive frequencies comparable to a few fractions of the photon frequency, as known in the context of the dynamical Casimir

effect. Generally, one understands that the production of virtual to real excitations must be done nonadiabatically, which means a sudden switch on and switch off of an interaction. Hence, it is expected that nonsmooth waveforms, such as a periodic array of sudden ramps (sawtooth) or top-hat functions, are comparatively highly productive [93]. These waveforms should not depend too much on ω_M , since the turn on and turn off is nonadiabatic, like how stimulated Raman adiabatic passage works best with a triangular pulse [94] (see [78]).

To conclude, we have investigated the dynamics of a cavity-QED system prepared initially in its lowest-dressed state subject to a time-dependent coupling rate in the USC regime, a Floquet engineered QRM. By using a suitable gauge-invariant model Hamiltonian, we described the generation of real excitations out of vacuum. This release of energy, which is initially stored in the form of virtual particles as a signature of the USC regime, is feasible by the nonadiabatic change in the system Hamiltonian, which is manifested by the mechanical oscillation of the location of the atom (or, also the cavity).

This work was supported by the Natural Sciences and Engineering Research Council of Canada (NSERC), the National Research Council of Canada (NRC), the Canadian Foundation for Innovation (CFI), and Queen's University, Canada. S.H. acknowledges the Japan Society for the Promotion of Science (JSPS) for funding support through an Invitational Fellowship. F.N. is supported in part by the Nippon Telegraph and Telephone Corporation (NTT) Research, the Japan Science and Technology Agency (JST) [via the Quantum Leap Flagship Program (Q-LEAP), and the Moonshot R&D Grant Number JP-MJMS2061], the Asian Office of Aerospace Research and Development (AOARD) (via Grant No. FA2386-20-1-4069), and the Office of Naval Research (ONR) Global (via Grant No. N62909-23-1-2074).

* kamran.akbari@queensu.ca

- [1] A. A. Anappara, S. De Liberato, A. Tredicucci, C. Ciuti, G. Biasiol, L. Sorba, and F. Beltram, Signatures of the ultrastrong light-matter coupling regime, *Physical Review B* **79**, 201303(R) (2009).
- [2] B. Zaks, D. Stehr, T.-A. Truong, P. M. Petroff, S. Hughes, and M. S. Sherwin, THz-driven quantum wells: Coulomb interactions and stark shifts in the ultrastrong coupling regime, *New Journal of Physics* **13**, 083009 (2011).
- [3] A. Frisk Kockum, A. Miranowicz, S. De Liberato, S. Savasta, and F. Nori, Ultrastrong coupling between light and matter, *Nature Reviews Physics* **1**, 19 (2019).
- [4] P. Forn-Díaz, L. Lamata, E. Rico, J. Kono, and E. Solano, Ultrastrong coupling regimes of light-matter interaction, *Rev. Mod. Phys.* **91**, 025005 (2019).
- [5] S. De Liberato, Virtual photons in the ground state of a dissipative system, *Nat Commun* **8**, 1465 (2017).
- [6] A. F. Kockum, A. Miranowicz, V. Macrì, S. Savasta, and F. Nori, Deterministic quantum nonlinear optics with single atoms and virtual photons, *Phys. Rev. A* **95**, 063849 (2017).
- [7] T. Werlang, A. V. Dodonov, E. I. Duzzioni, and C. J. Villas-Bôas, Rabi model beyond the rotating-wave approximation: Generation of photons from vacuum through decoherence, *Phys. Rev. A* **78**, 053805 (2008).
- [8] M. Cirio, K. Debnath, N. Lambert, and F. Nori, Amplified optomechanical transduction of virtual radiation pressure, *Phys. Rev. Lett.* **119**, 053601 (2017).
- [9] C. Ciuti, G. Bastard, and I. Carusotto, Quantum vacuum properties of the intersubband cavity polariton field, *Physical Review B* **72**, 115303 (2005).
- [10] P. D. Nation, J. R. Johansson, M. P. Blencowe, and F. Nori, Colloquium: Stimulating uncertainty: Amplifying the quantum vacuum with superconducting circuits, *Rev. Mod. Phys.* **84**, 1 (2012).
- [11] J. Lolli, A. Baksic, D. Nagy, V. E. Manucharyan, and C. Ciuti, Ancillary Qubit Spectroscopy of Vacua in Cavity and Circuit Quantum Electrodynamics, *Phys. Rev. Lett.* **114**, 183601 (2015).
- [12] A. Ridolfo, J. Rajendran, L. Giannelli, E. Paladino, and G. Falci, Probing ultrastrong light-matter coupling in open quantum systems, *The European Physical Journal Special Topics* **230**, 941 (2021).
- [13] S. D. Liberato, C. Ciuti, and I. Carusotto, Quantum vacuum radiation spectra from a semiconductor microcavity with a time-modulated vacuum rabi frequency, *Phys. Rev. Lett.* **98**, 103602 (2007).
- [14] K. Takashima, N. Hatakenaka, S. Kurihara, and A. Zeilinger, Nonstationary boundary effect for a quantum flux in superconducting nanocircuits, *Journal of Physics A: Mathematical and Theoretical* **41**, 164036 (2008).
- [15] A. V. Dodonov, L. C. Celeri, F. Pascoal, M. D. Lukin, and S. F. Yelin, Photon generation from vacuum in nonstationary circuit QED (2008), [arXiv:0806.4035 \[quant-ph\]](https://arxiv.org/abs/0806.4035).
- [16] A. V. Dodonov, Photon creation from vacuum and interactions engineering in nonstationary circuit QED, *Journal of Physics: Conference Series* **161**, 012029 (2009).
- [17] F. Beaudoin, J. M. Gambetta, and A. Blais, Dissipation and ultrastrong coupling in circuit QED, *Phys. Rev. A* **84**, 043832 (2011).
- [18] S. de Liberato, D. Gerace, I. Carusotto, and C. Ciuti, Extracavity quantum vacuum radiation from a single qubit, *Physical Review A : Atomic, molecular, and optical physics [1990-2015]* **80**, 053810 (2009).
- [19] I. Carusotto, S. De Liberato, D. Gerace, and C. Ciuti, Back-reaction effects of quantum vacuum in cavity quantum electrodynamics, *Phys. Rev. A* **85**, 023805 (2012).
- [20] L. Garziano, A. Ridolfo, R. Stassi, O. Di Stefano, and S. Savasta, Switching on and off of ultrastrong light-matter interaction: Photon statistics of quantum vacuum radiation, *Phys. Rev. A* **88**, 063829 (2013).
- [21] D. S. Shapiro, A. A. Zhukov, W. V. Pogosov, and Y. E. Lozovik, Dynamical Lamb effect in a tunable superconducting qubit-cavity system, *Phys. Rev. A* **91**, 063814 (2015).
- [22] G. Günter, A. A. Anappara, J. Hees, A. Sell, G. Biasiol, L. Sorba, S. De Liberato, C. Ciuti, A. Tredicucci, A. Leitenstorfer, and R. Huber, Sub-cycle switch-on of ultrastrong light-matter interaction, *Nature* **458**, 178 (2009).

- [23] A. Ridolfo, R. Vilaridi, O. Di Stefano, S. Portolan, and S. Savasta, All optical switch of vacuum rabi oscillations: The ultrafast quantum eraser, *Phys. Rev. Lett.* **106**, 013601 (2011).
- [24] J.-F. Huang and C. K. Law, Photon emission via vacuum-dressed intermediate states under ultrastrong coupling, *Phys. Rev. A* **89**, 033827 (2014).
- [25] M. Cirio, S. De Liberato, N. Lambert, and F. Nori, Ground state electroluminescence, *Phys. Rev. Lett.* **116**, 113601 (2016).
- [26] F. Minganti, A. Mercurio, F. Mauceri, M. Scigliuzzo, S. Savasta, and V. Savona, Phonon Pumping by Modulating the Ultrastrong Vacuum, (2023), [arXiv:2309.15891](https://arxiv.org/abs/2309.15891) [quant-ph].
- [27] A. Mercurio, S. D. Liberato, F. Nori, S. Savasta, and R. Stassi, Flying atom back-reaction and mechanically generated photons from vacuum (2022), [arXiv:2209.10419](https://arxiv.org/abs/2209.10419) [quant-ph].
- [28] V. Macrì, A. Ridolfo, O. Di Stefano, A. F. Kockum, F. Nori, and S. Savasta, Nonperturbative Dynamical Casimir Effect in Optomechanical Systems: Vacuum Casimir-Rabi Splittings, *Physical Review X* **8**, 011031 (2018).
- [29] J. R. Johansson, G. Johansson, C. M. Wilson, and F. Nori, Dynamical casimir effect in a superconducting coplanar waveguide, *Phys. Rev. Lett.* **103**, 147003 (2009).
- [30] J. R. Johansson, G. Johansson, C. M. Wilson, and F. Nori, Dynamical casimir effect in superconducting microwave circuits, *Phys. Rev. A* **82**, 052509 (2010).
- [31] J. R. Johansson, G. Johansson, C. M. Wilson, P. Delsing, and F. Nori, Nonclassical microwave radiation from the dynamical casimir effect, *Phys. Rev. A* **87**, 043804 (2013).
- [32] C. M. Wilson, G. Johansson, A. Pourkabirian, M. Simoen, J. R. Johansson, T. Duty, F. Nori, and P. Delsing, Observation of the dynamical Casimir effect in a superconducting circuit, *Nature* **479**, 10.1038/nature10561 (2011), publisher: Nature Publishing Group.
- [33] D. A. R. Dalvit, Shaking photons out of the vacuum, *Nature* **479**, 303 (2011), publisher: Nature Publishing Group.
- [34] O. Di Stefano, A. Settineri, V. Macrì, A. Ridolfo, R. Stassi, A. F. Kockum, S. Savasta, and F. Nori, Interaction of mechanical oscillators mediated by the exchange of virtual photon pairs, *Phys. Rev. Lett.* **122**, 030402 (2019).
- [35] A. Settineri, V. Macrì, L. Garziano, O. Di Stefano, F. Nori, and S. Savasta, Conversion of mechanical noise into correlated photon pairs: Dynamical casimir effect from an incoherent mechanical drive, *Phys. Rev. A* **100**, 022501 (2019).
- [36] W. Qin, V. Macrì, A. Miranowicz, S. Savasta, and F. Nori, Emission of photon pairs by mechanical stimulation of the squeezed vacuum, *Phys. Rev. A* **100**, 062501 (2019).
- [37] D. De Bernardis, P. Pilar, T. Jaako, S. De Liberato, and P. Rabl, Breakdown of gauge invariance in ultrastrong-coupling cavity QED, *Phys. Rev. A* **98**, 053819 (2018).
- [38] W. Salmon, C. Gustin, A. Settineri, O. D. Stefano, D. Zueco, S. Savasta, F. Nori, and S. Hughes, Gauge-independent emission spectra and quantum correlations in the ultrastrong coupling regime of open system cavity-QED, *Nanophotonics* **11**, 1573 (2022).
- [39] K. Akbari, W. Salmon, F. Nori, and S. Hughes, Generalized Dicke model and gauge-invariant master equations for two atoms in ultrastrongly-coupled cavity quantum electrodynamics, *Phys. Rev. Res.* **5**, 033002 (2023).
- [40] A. Settineri, V. Macrì, A. Ridolfo, O. Di Stefano, A. F. Kockum, F. Nori, and S. Savasta, Dissipation and thermal noise in hybrid quantum systems in the ultrastrong-coupling regime, *Phys. Rev. A* **98**, 053834 (2018).
- [41] O. Di Stefano, A. Settineri, V. Macrì, L. Garziano, R. Stassi, S. Savasta, and F. Nori, Resolution of gauge ambiguities in ultrastrong-coupling cavity quantum electrodynamics, *Nat. Phys.* **15**, 803 (2019).
- [42] M. A. D. Taylor, A. Mandal, W. Zhou, and P. Huo, Resolution of gauge ambiguities in molecular cavity quantum electrodynamics, *Phys. Rev. Lett.* **125**, 123602 (2020).
- [43] M. A. D. Taylor, A. Mandal, and P. Huo, Resolving ambiguities of the mode truncation in cavity quantum electrodynamics, *Optics Letters* **47**, 1446 (2022).
- [44] A. Settineri, O. Di Stefano, D. Zueco, S. Hughes, S. Savasta, and F. Nori, Gauge freedom, quantum measurements, and time-dependent interactions in cavity QED, *Phys. Rev. Res.* **3**, 023079 (2021).
- [45] C. Gustin, S. Franke, and S. Hughes, Gauge-invariant theory of truncated quantum light-matter interactions in arbitrary media, *Phys. Rev. A* **107**, 013722 (2023).
- [46] V. Macrì, A. Mercurio, F. Nori, S. Savasta, and C. Sánchez Muñoz, Spontaneous scattering of Raman photons from cavity-qed systems in the ultrastrong coupling regime, *Phys. Rev. Lett.* **129**, 273602 (2022).
- [47] G. Floquet, Sur les équations différentielles linéaires à coefficients périodiques, *Annales scientifiques de l'École Normale Supérieure* **12**, 47 (1883).
- [48] M. Grifoni and P. Hänggi, Driven quantum tunneling, *Physics Reports* **304**, 229 (1998).
- [49] T. Iadecola and C. Chamon, Floquet systems coupled to particle reservoirs, *Phys. Rev. B* **91**, 184301 (2015).
- [50] T. Oka and S. Kitamura, Floquet engineering of quantum materials, *Annual Review of Condensed Matter Physics* **10**, 387 (2019), <https://doi.org/10.1146/annurev-conmatphys-031218-013423>.
- [51] O. R. Diermann and M. Holthaus, Floquet-state cooling, *Sci Rep* **9**, 17614 (2019), number: 1 Publisher: Nature Publishing Group.
- [52] C. Weitenberg and J. Simonet, Tailoring quantum gases by Floquet engineering, *Nat. Phys.* **17**, 1342 (2021), number: 12 Publisher: Nature Publishing Group.
- [53] J. N. Bandyopadhyay and J. Thingna, Floquet engineering of lie algebraic quantum systems, *Phys. Rev. B* **105**, L020301 (2022).
- [54] F. Petziol and A. Eckardt, Cavity-based reservoir engineering for Floquet-engineered superconducting circuits, *Phys. Rev. Lett.* **129**, 233601 (2022).
- [55] H. Liu, H. Cao, and S. Meng, Floquet engineering of topological states in realistic quantum materials via light-matter interactions, *Progress in Surface Science* **98**, 100705 (2023).
- [56] A. Castro, U. D. Giovannini, S. A. Sato, H. Hübener, and A. Rubio, Floquet engineering with quantum optimal control theory, *New Journal of Physics* **25**, 043023 (2023).
- [57] F. Zhan, J. Zeng, Z. Chen, X. Jin, J. Fan, T. Chen, and R. Wang, Floquet Engineering of Nonequilibrium Valley-Polarized Quantum Anomalous Hall Effect with Tunable Chern Number, *Nano Lett.* **23**, 2166 (2023), publisher: American Chemical Society.
- [58] S. Geier, N. Thaicharoen, C. Hainaut, T. Franz, A. Salzinger, A. Tebben, D. Grimshandl,

- G. Zürn, and M. Weidemüller, Floquet Hamiltonian engineering of an isolated many-body spin system, *Science* **374**, 1149 (2021), <https://www.science.org/doi/pdf/10.1126/science.abd9547>.
- [59] S.-Y. Bai and J.-H. An, Floquet Engineering to Overcome No-Go Theorem of Noisy Quantum Metrology, *Phys. Rev. Lett.* **131**, 050801 (2023), arXiv:2303.00392 [quant-ph].
- [60] A. Schnell, C. Weitenberg, and A. Eckardt, Dissipative preparation of a Floquet topological insulator in an optical lattice via bath engineering (2023), arXiv:2307.03739 [cond-mat.quant-gas].
- [61] U. Kumar, S. Banerjee, and S.-Z. Lin, Floquet engineering of Kitaev quantum magnets, *Commun Phys* **5**, 1 (2022), number: 1 Publisher: Nature Publishing Group.
- [62] P. K. Tien and J. P. Gordon, Multiphoton process observed in the interaction of microwave fields with the tunneling between superconductor films, *Phys. Rev.* **129**, 647 (1963).
- [63] F. Grossmann, T. Dittrich, P. Jung, and P. Hänggi, Coherent destruction of tunneling, *Phys. Rev. Lett.* **67**, 516 (1991).
- [64] G. Platero and R. Aguado, Photon-assisted transport in semiconductor nanostructures, *Physics Reports* **395**, 1 (2004).
- [65] A. Eckardt, T. Jinasundera, C. Weiss, and M. Holthaus, Analog of photon-assisted tunneling in a Bose-Einstein condensate, *Phys. Rev. Lett.* **95**, 200401 (2005).
- [66] K. Shibata, A. Umeno, K. M. Cha, and K. Hirakawa, Photon-assisted tunneling through self-assembled InAs quantum dots in the terahertz frequency range, *Phys. Rev. Lett.* **109**, 077401 (2012).
- [67] W. A. Coish and J. M. Gambetta, Entangled photons on demand: Erasing which-path information with sidebands, *Phys. Rev. B* **80**, 241303 (2009).
- [68] P. Delsing, A. N. Cleland, M. J. A. Schuetz, J. Knörzer, G. Giedke, J. I. Cirac, K. Srinivasan, M. Wu, K. C. Balram, C. Bäuerle, T. Meunier, C. J. B. Ford, P. V. Santos, E. Cerda-Méndez, H. Wang, H. J. Krenner, E. D. S. Nysten, M. Weiß, G. R. Nash, L. Thevenard, C. Gourdon, P. Rivillain, M. Marangolo, J.-Y. Duquesne, G. Fischerauer, W. Ruile, A. Reiner, B. Paschke, D. Denysenko, D. Volkmer, A. Wixforth, H. Bruus, M. Wiklund, J. Reboud, J. M. Cooper, Y. Fu, M. S. Brugger, F. Rehfeldt, and C. Westerhausen, The 2019 surface acoustic waves roadmap, *Journal of Physics D: Applied Physics* **52**, 353001 (2019).
- [69] F. Iikawa, A. Hernández-Mínguez, M. Ramsteiner, and P. V. Santos, Optical phonon modulation in semiconductors by surface acoustic waves, *Phys. Rev. B* **93**, 195212 (2016).
- [70] P. Roelli, C. Galland, N. Piro, and T. J. Kippenberg, Molecular cavity optomechanics as a theory of plasmon-enhanced Raman scattering, *Nature Nanotechnology* **11**, 164 (2015).
- [71] M. K. Schmidt, R. Esteban, A. González-Tudela, G. Giedke, and J. Aizpurua, Quantum mechanical description of Raman scattering from molecules in plasmonic cavities, *ACS Nano* **10**, 6291 (2016).
- [72] M. K. Dezfouli, R. Gordon, and S. Hughes, Molecular optomechanics in the anharmonic cavity-QED regime using hybrid metal-dielectric cavity modes, *ACS Photonics* **6**, 1400 (2019).
- [73] M. Abramowitz and I. Stegun, *Handbook of Mathematical Functions: With Formulas, Graphs, and Mathematical Tables*, Applied mathematics series (Dover Publications, 1965).
- [74] S. Ashhab, J. R. Johansson, A. M. Zagoskin, and F. Nori, Two-level systems driven by large-amplitude fields, *Phys. Rev. A* **75**, 063414 (2007).
- [75] A. I. Nikishov and V. I. Ritus, Quantum Processes in the Field of a Plane Electromagnetic Wave and in a Constant Field 1, *Sov. Phys. JETP* **19**, 529 (1964).
- [76] C. Chicone, *Ordinary Differential Equations with Applications*, Texts in Applied Mathematics (Springer New York, 2006).
- [77] J. H. Shirley, Solution of the Schrödinger equation with a Hamiltonian periodic in time, *Phys. Rev.* **138**, B979 (1965).
- [78] See supplemental material at <https://link.aps.org/doi/10.1103/PhysRevLett.119.053601> for [give brief description of material].
- [79] S. Chu, J. V. Tietz, and K. K. Datta, Quantum dynamics of molecular multiphoton excitation in intense laser and static electric fields: Floquet theory, quasienergy spectra, and application to the HF molecule, *The Journal of Chemical Physics* **77**, 2968 (1982).
- [80] S.-I. Chu, Recent Developments in Semiclassical Floquet Theories for Intense-Field Multiphoton Processes (Academic Press, 1985) pp. 197–253, iSSN: 0065-2199.
- [81] S.-I. Chu and D. A. Telnov, Beyond the Floquet theorem: generalized Floquet formalisms and quasienergy methods for atomic and molecular multiphoton processes in intense laser fields, *Physics Reports* **390**, 1 (2004).
- [82] T.-S. Ho, K. Wang, and S.-I. Chu, Floquet-Liouville supermatrix approach: Time development of density-matrix operator and multiphoton resonance fluorescence spectra in intense laser fields, *Phys. Rev. A* **33**, 1798 (1986).
- [83] H. P. Breuer and M. Holthaus, Adiabatic processes in the ionization of highly excited hydrogen atoms, *Zeitschrift für Physik D Atoms, Molecules and Clusters* **11**, 1 (1989).
- [84] H. Breuer and M. Holthaus, *Quantum phases and Landau-Zener transitions in oscillating fields*, Tech. Rep. (Germany, 1989) bONN-AM-89-04 INIS Reference Number: 20077409.
- [85] M. Holthaus, Floquet engineering with quasienergy bands of periodically driven optical lattices, *Journal of Physics B: Atomic, Molecular and Optical Physics* **49**, 013001 (2015).
- [86] S. Hughes, C. Gustin, and F. Nori, Reconciling quantum and classical spectral theories of ultrastrong coupling: role of cavity bath coupling and gauge corrections, *Optica Quantum* **2**, 133 (2024).
- [87] A. Eckardt, Colloquium: Atomic quantum gases in periodically driven optical lattices, *Rev. Mod. Phys.* **89**, 011004 (2017).
- [88] N. Vitanov, B. Shore, L. Yatsenko, K. Böhmer, T. Halfmann, T. Rickes, and K. Bergmann, Power broadening revisited: theory and experiment, *Optics Communications* **199**, 117 (2001).
- [89] S. H. Autler and C. H. Townes, Stark effect in rapidly varying fields, *Phys. Rev.* **100**, 703 (1955).
- [90] C. N. Cohen-Tannoudji, The Autler-Townes effect revisited, in *Amazing Light: A Volume Dedicated To Charles Hard Townes On His 80th Birthday* (Springer, 1996) pp. 109–123.
- [91] E. H. Ahmed, J. Huennekens, T. Kirova, J. Qi, and

- A. M. Lyyra, The Autler–Townes effect in molecules: Observations, theory, and applications, in *Advances in Atomic, Molecular, and Optical Physics*, Advances In Atomic, Molecular, and Optical Physics, Vol. 61, edited by P. Berman, E. Arimondo, and C. Lin (Academic Press, 2012) pp. 467–514.
- [92] B. Peng, S. K. Özdemir, W. Chen, F. Nori, and L. Yang, What is and what is not electromagnetically induced transparency in whispering-gallery microcavities, *Nature Communications* **5**, 5082 (2014), publisher: Nature Publishing Group.
- [93] K. Ono, S. N. Shevchenko, T. Mori, S. Moriyama, and F. Nori, Quantum interferometry with a g -factor-tunable spin qubit, *Phys. Rev. Lett.* **122**, 207703 (2019).
- [94] K. Drese and M. Holthaus, Floquet theory for short laser pulses, *Eur. Phys. J. D* **5**, 119 (1999).